Strategic Astrophysics Technology

Technology Milestone Whitepaper

Thermo-Optical Metrology for Exoplanet observatories (TOMEx)

Felipe Guzmán, Moritz Mehmet, Jose Sanjuan

August 19, 2025

Prepared by:

E-SIGNED by Felipe Guzman
on 2025-08-19 19:53:22 GMT

Felipe Guzmán
Principal Investigator
University of Arizona

Date

Approved by:

E-SIGNED by Brendan Crill
on 2025-08-19 19:53:35 GMT

Brendan Crill
ExEP Deputy Program Chief Technologist

Date

E-SIGNED by Nicholas Siegler
on 2025-08-19 20:25:03 GMT

Nick Siegler
ExEP Program Chief Technologist

Date

E-SIGNED by Lucas Paganini
on 2025-08-19 20:31:05 GMT

Lucas Paganini
ExEP Program Executive, NASA-HQ

Date

Table of Contents

1. Objectives

NASA's Exoplanet Exploration Program (ExEP) aims to search for habitable planets and life beyond our solar system. Following the recommendation of the 2020 Decadal Survey on Astronomy and Astrophysics [1], NASA's Habitable Worlds Observatory (HWO) is envisioned as a 6-meter aperture space telescope equipped with advanced starlight suppression capabilities. HWO builds on key technologies and design concepts from previous mission studies, including LUVOIR (Large Ultraviolet Optical Infrared Surveyor) and HabEx (Habitable Exoplanet Observatory), to enable direct imaging and atmospheric characterization of Earth-like exoplanets. The signatures of Earth-like planets are much weaker than those coming from the stars they orbit. The brightness difference depends on the wavelength. For mid-infrared the required contrast is about 10^7, while in the visible it goes up to 10^{10}. Therefore, the starlight suppression must be of ten orders of magnitude to detect from the reflected light of the planet the presence of water, methane, and oxygen in its atmosphere. Such starlight suppression poses significant technological challenges to prevent the *signal from the bright star* from dominating the planetary signal. Among others, a critical aspect is the stability of the space telescope, which translates into stringent wavefront error requirements.

Wavefront error mitigation in large telescopes requires a combination of advancements in technology as listed in the ExoPlanet Exploration Program (ExEP) Technology Gap List [2]. They include ultra-stable telescope structures, disturbance reduction systems (platform stability), wavefront sensing metrology both in-band and long-term, vibration isolation, laser gauges for metrology, segment relative position and orientation sensing, and thermal sensing and control.

The work proposed here will aid in the maturation of technology related to thermal sensing and control, laser gauges for metrology, wavefront sensing, and segment relative position/orientation metrology. Specifically, our project aims to:

- **Demonstrate tens of micro-Kelvin temperature stability environment.**
- **Demonstrate picometer precision with long-baseline optical truss interferometers.**
- **Demonstrate picometer/nanoradian segment position and orientation sensing.**
- **Demonstrate wavefront error sensing at the picometer level using per-pixel heterodyne interferometry phase extraction with a CCD camera.**
- **Test all these technologies in a coherent set-up with a mock-up telescope for requirements and model validation.**

The Technology Readiness Level (TRL) of the technologies proposed here is at different levels. Our goal is to increase them by one step for each of the four technologies (corresponding to the first four bullet points above). Our assessment of the TRLs is summarized in Table 1 below. At this stage, the main goal of the proposed technology is to demonstrate performance compatible with HWO needs in laboratory environments.

Future developments will further increase the technologies' maturity for integration into HWO missions.

Table 1. TRL input and output levels for the proposed technology development.

Technology	TRL in	TRL out	Comments
Thermal sensing and control	4	5	The thermal sensing and control at the μK level as a system for a rather large telescope structure is considered at TRL 4. The successful combination of high sensitivity sensors together with active and passive control will elevate the TRL to 5.
Laser gauges for telescope dimensional stability measurements	4	5	We have developed similar technology within the framework of the LISA mission. Low-fidelity systems have been demonstrated in the laboratory
Segment position and orientation systems	3	4	We have developed compact interferometers suitable for measuring the individual segments of a telescope. While the systems can be upgradable for angle measurements, it needs development and testing.
Wavefront sensing	3	4	Wavefront sensing based on CCD cameras and heterodyne interferometry have been demonstrated in the laboratory at the sub-nanometer level.

2. Introduction and background

The work proposed here is relevant to improve Coronagraph Contrast Stability, which is one of the identified technology gaps within the ExoPlanets Exploration Program [1,2]. Coronagraph stability refers to the need of maintaining high and stable contrast to perform spectral measurements of Earth-like planets orbiting bright stars. To do so, the telescope's wavefront error must be at the 10-100 pm level for a few minutes. Such requirement is about 3 orders of magnitude more stringent than JWST or the LISA telescope. JWST exhibits wavefront errors around 20 nm on time scales of two days and it is limited by relative segment motion [3], while the LISA telescope, currently under NASA development, aims for 35 nm wavefront errors [4]. Thermal effects, mechanical vibrations, and inherent material creep are some of the disturbances that can degrade wavefront quality, and thus need to be mitigated by a combination of passive and active measures. Some mitigating and correcting measures are listed below:

- Ultra-stable thermal sensing and control,
- optical metrology to measure the distance between the primary and secondary mirrors of the telescope,
- metering interferometers to measure relative motion between segments, and

- wavefront sensing capabilities at the pico-meter level.

We will develop technologies to cover these four aspects, which align with the technology sub-gaps identified by the ExEP to address coronagraph contrast and telescope stability [1].

Stable thermal sensing and control

Wavefront errors and temperature fluctuations are strongly related. The latter causes mechanical distortions due to non-zero coefficient of thermal expansion (CTE), which ultimately translates into wavefront errors due to deviations from the nominal design [5]. The coupling coefficient between temperature fluctuations and wavefront errors is not straightforward and requires detailed opto-thermomechanical simulations. Nevertheless, the expected coefficients are in the order of few pm/mK [1]. Thus, pico-meter wavefront error stability requires milli-Kelvin thermal stability, which is challenging for long time scales and in rather large optical systems.

The current state-of-the-art for thermal sensing and control is at the mK level for a 1.5 m ULE mirror. It has been demonstrated by work at NASA/MSFC in a vacuum environment [5]. The system uses temperature sensors with noise in the 50 mK range, and heaters in a multizone thermal control. We propose the development of thermometers with noise levels at micro-Kelvin level, which, in turn, will allow to achieve better thermal environments since ideally any active control is ultimately limited by the sensor noise. While temperature sensor noise is crucial for the thermal control design, the control itself poses important challenges due to several reasons such as, for example, the inherent low bandwidth of the actuators that limits the gain of the controllers, the asymmetry of the actuators unless Peltier elements (i.e., thermoelectrical coolers, TECs, which allow for bidirectional heat transfer depending on the direction of the current) are used (which, in turn, create other challenges), and the need to infer a temperature map from a few sensing points.

We have faced similar challenges in other missions where thermal environments at the micro-Kelvin level for time scales of hours were necessary. In LISA Pathfinder [6], the successful LISA technology demonstrator, sensing noise was required at the 10 μK/√Hz level from 1 mHz to 1 Hz [7], which translates to a rms value of 300 nK on time scales of 10 minutes. LISA requires a ten-fold sensitivity improvement, which we have also demonstrated in the laboratory [8]. The development and testing of such technology have also forced us to develop extremely stable thermal environments both with passive and active controls. Finally, development of a high-finesse ultra-stable optical cavity for testing of fundamental physics in space required the thermal stabilization of a 10-cm optical cavity down to 0.1 μK/√Hz at 0.2 mHz [9], which in terms of rms is a few nK. Such stability was also demonstrated by a combination of active control (using Peltier elements) and thermal shields.

Optical metrology to measure distance changes between primary and secondary mirrors of the telescope

Relative motion between the primary and secondary mirrors of the telescope will introduce wavefront errors in the telescope. Thus, such motions need to be measured and corrected. This is a similar problem encountered in the LISA telescope, where picometer stability between the primary and secondary is required [10,11]. An attractive solution to measure such small length changes is optical trusses based on optical cavities [12]. It has been shown that high-finesse optical cavities can provide precise length measurements at the fm/√Hz level [9]. For moderate finesse optical cavities, the noise levels can be well below pm/√Hz. This approach is being developed as a risk mitigation strategy in LISA and could be adapted for the HWO mission. Several laser gauges can be implemented using a single laser head together with optical cavities and frequency side-band locking [13,14]. In this scheme, it is important that the laser head is frequency stabilized to a highly stable frequency reference, e.g., an optical cavity [9] or a spectroscopy unit [15]. The former performs better at short time scales, while the latter provides an absolute frequency reference with excellent long-term stability. In both cases, 0.1 pm/√Hz noise levels should be possible, which corresponds to rms levels of 3 fm on time scales of 20-30 minutes, and 0.1 pm at short time scales, 1 second.

Metering interferometers to measure relative motion between segments

The relative position and orientation of the segments in segmented primary mirrors of space telescopes is important to minimize wavefront errors and keep the telescope aligned. This is especially true for wavefront error requirements at the picometer level. The relative position and orientation can be measured by probing the back of the segments from the telescope primary mirror frame with heterodyne laser interferometry [16]. Small, compact, and rugged interferometer heads can be deployed around the segments of the primary mirror. Each of the sensor's heads will be able to measure both longitudinal and orientation changes by means of quadrant photodetectors and differential wavefront sensing [17]. Heterodyne interferometric measurements allow for sub-pm and nano-radian precision measurements [18], and thus are adequate for the HWO needs. A key aspect of the system is the possibility of upscaling it to many sensor heads (as many as telescope segments), which we have already explored for multi-axial accelerometers, where several degrees of freedom must be measured simultaneously.

Wavefront sensing capabilities at the pm level

Direct measurement of the wavefront error with high spatial resolution and high sensitivity has been a persistent challenge in the development of high performing optics in space telescopes for both monolithic and segmented systems. Typical approaches to conduct such wavefront measurements involve the use of Shack-Hartmann or pyramid wavefront sensors [19] that can achieve measurement sensitivities in the order of 10s of mrad in the resulting wavefront error upon conducting a variety of corrections. Other alternatives involve the use of laser interferometry such as the established Zygo instruments [20] that, however, require a careful actuation on the beam position to measure the object under test, thus limiting the spatial resolution.

We will develop a laser-interferometric wavefront sensor that allows us to achieve high-sensitivity high-spatially resolved measurements by conducting interferometric phase

retrieval per pixel on a high-resolution fast CCD camera. The development will target significant improvements upon technology previously developed [21].

Clarification on spectral densities and RMS values:
The relationship between Power Spectral Density (PSD), $S(f)$, and variance, σ^2, is as follows:

$$\sigma^2 = \int_{f_m}^{f_M} S(f) df$$

where f_m and f_M are the lowest and highest frequencies of interest, respectively. Note the PSD has units of unit^2/Hz, and the variance has units of unit^2. Naturally, their square-rooted versions have units of unit/rtHz and unit. The RMS value is simply the square-rooted version of the variance.

We have defined the measurement bandwidth from 10 mHz to 10 Hz. In other words, from time scales of 100 seconds to 0.1 seconds. We have defined our goals/requirements in terms of RMS values, to better align with reported HWO requirements and figures of merit.

3. Technical Approach

The project has well-identified activities, which correspond to the four technology gaps listed above. In the following, we describe them in detail. The ultimate goal is to test all the technologies within a relevant environment where temperature stability and optical metrology can be demonstrated together. Furthermore, the setup will be used for wavefront error model validation and correlation using a mock-up telescope.

3.1 Thermal sensing and control

Thermal sensing will be based on thermistors together with ultra-low-noise electronics. The measuring concept will be based on a thermistor in an AC Wheatstone bridge configuration, sampled by multi-channel 24-bit analog-to-digital converters (ADC), followed by digital demodulation in an FPGA. A similar concept has been used in LISA Pathfinder and will be used in LISA to measure micro-Kelvin fluctuations [22].

Ultimately, the sensitivity is limited by the thermal noise of the Wheatstone bridge resistors and thermistors, which can be reduced to some extent by increasing the power dissipated in the sensor head. The power dissipated in the temperature sensors will be in the order of 10-100 μW, which we expect will have no effect on the telescope's optics and structure. At most, small hot spots (few mK increase above the average temperature) will be present. Nevertheless, it is part of the project to evaluate the effect and impact of the power dissipated in the temperature sensors.

Thermal stability will be achieved by including active control and passive thermal shielding. The latter attenuates thermal fluctuations at short time scales due to the low-pass filtering nature of the thermal mass, while the former takes care of low-frequency

variations, which are difficult to dampen by passive elements. A combination of thermal shields/baffles together with the mass of the telescope's mirror will damp temperature fluctuations well below the milli-Kelvin at short time scales (<100-1,000 s). The design will be driven by the required attenuation, which ultimately depends on the expected thermal environment. Initially, analytical calculations in the frequency domain will provide us with a good estimate of the needs of passive shielding. Analytical calculations will be refined using finite-element computations with commercial software. The active control will be designed by choosing optimal actuators (probably Kapton resistive heaters) together with multi-zone control strategies to maximize thermal stability and minimize thermal gradients across the telescope. Figure 1 shows the attenuation (as transfer functions) to external temperature fluctuations when using an active control together with passive shielding. The former reduces fluctuations in the low-frequency regime, while the latter strongly attenuates fluctuations at short time scales, where the controller typically has little authority due to the low bandwidth of the actuators. The thermal sensing and the controller, once assembled, tested, and characterized, will be installed in a thermal-vacuum chamber together with a mock-up telescope for testing.

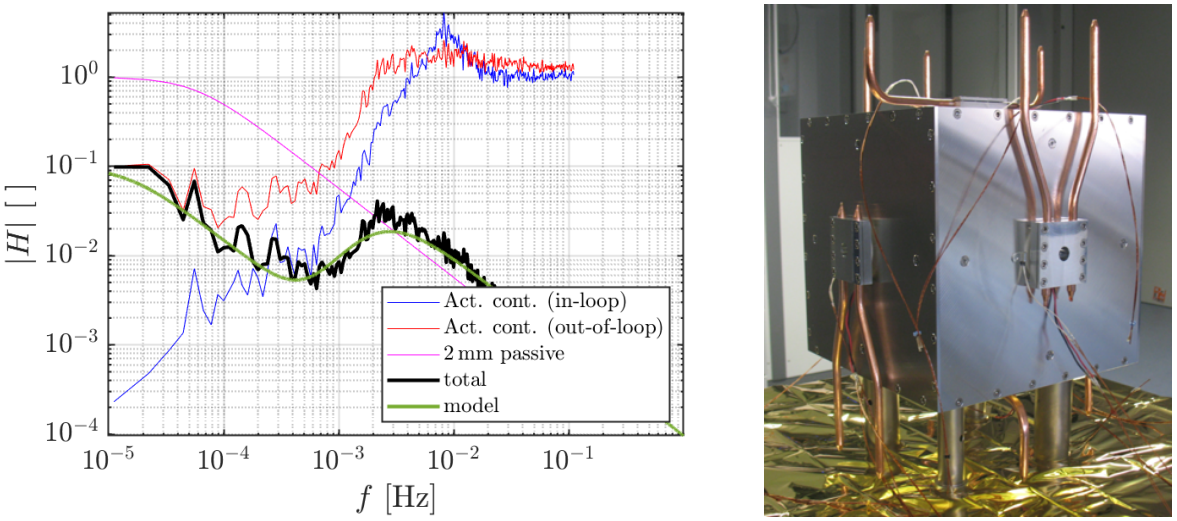

Figure 1. Left: attenuation transfer function for active control (red trace) and passive shielding (magenta) predicted for the LISA telescope picometer stability testing. Combination of both systems yields the optimal trace (black and green). Attenuation transfer function refers to the relationship between input and output temperature fluctuations of the system in the frequency domain. For instance, the green trace on the left plot (model) shows that temperature fluctuations at 10^{-5} Hz (~1 day period) are only attenuated by 10%, while faster fluctuations are strongly attenuated. For instance, at 1 mHz (time scales of 15 minutes) temperature fluctuations are attenuated by two orders of magnitude. The attenuation transfer function is a property of the system and, thus, can be used for any external temperature fluctuations to estimate the fluctuations after the filter. Right: thermal shields and Peltier actuators (plus heat pipes) for ultra-stable long-term optical cavity set-up for tests of fundamental physics in space [9].

3.2 Optical trusses

We have already developed a modular optical truss interferometer (OTI), which is based on a two-mirror cavity setup [12,23], and aims to provide support for ground testing of the LISA telescopes, as well as a risk-mitigation plan for the flight units. Building on our previous work, we will develop optical truss interferometers tailored for a possible HWO telescope to measure its dimensional stability. Compared to our previously demonstrated OTIs, we envision a size reduction of the input and return stage, respectively, and the increase of the nominal cavity length to distances beyond the current operating range of 0.7 m. The goal is to measure picometer length changes of distances between the input and output stages of up to 3 m. In addition, we will assess the feasibility of extending the measurement range to distances of around 15 m. The core of the OTI will be a compact input stage that comprises the components for injecting a laser beam, mode matching optics, and the cavity input mirror. The return stage will have a similar mechanical design but only houses the highly reflective cavity return mirror and, consequently, is much more compact. The input stage, paired with the return stage, can be mounted to a telescope (or any other structure) to form an optical truss cavity. For the devices described in [12], a reflectivity of 99.8% was chosen for both the cavity input and return mirror yielding a finesse of approximately 1,600, which was high enough to achieve sub-picometer precision. A possible implementation of three OTIs on a telescope is depicted in Fig. 2.

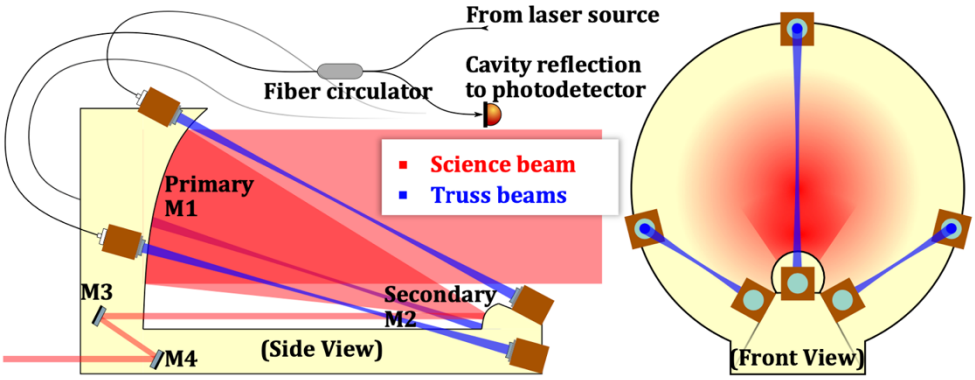

Figure 2. Side view and front view of a possible implementation of 3 OTIs on a telescope structure [12]. The fiber-injected input stages are attached around the primary mirror, while the return stages are attached around the secondary mirror.

To track the length changes of the OTI cavity, a laser will be locked to one of its resonance frequencies with a frequency-offset side-band locking [13,14] scheme based on the Pound-Drever-Hall (PDH) technique [24,25]. Once the lock is established by feeding back the error signal to the laser impinging on the cavity, changes in cavity length will be tracked by the required actuation signal, since $\delta L/L = \delta\nu/\nu$, where L is the optical length of the cavity, υ is the nominal laser frequency, and δ denotes fluctuations of these quantities. In such a scheme, however, a change of the laser frequency itself is undistinguishable from a change of cavity length. Therefore, our scheme requires an ultra-stable laser source to probe tiny length variations. We will use an iodine-stabilized laser system, which should allow us to sense sub-pm length changes of distances

between the input and output stages of up to 3 m. To facilitate even larger operating ranges and/or to improve the sensing noise floor for a given operating distance we plan to add a highly stable reference cavity to our system.

3.3 Compact interferometers for measuring segment position and orientation

Compact interferometers are excellent candidates to measure the relative position of segments of space telescopes at the sub-picometer and nano-radian levels. Heterodyne interferometry has been demonstrated in space at the tens of femto-meter level and tens of nano-radians [26]. While this was flown in LISA Pathfinder on an ultra-stable optical bench, laboratory demonstrators with much simpler set-ups have also shown noise levels in the 100 fm level. We have developed compact interferometers as part of low-frequency opto-mechanical accelerometers, see for example Refs. [27,28]. We will advance this development further to extend the sensing capabilities. Figure 3 shows a sketch of the interferometric beam paths (top) and a potential use of multiple interferometers on the structure of a segmented telescope mirror (bottom).

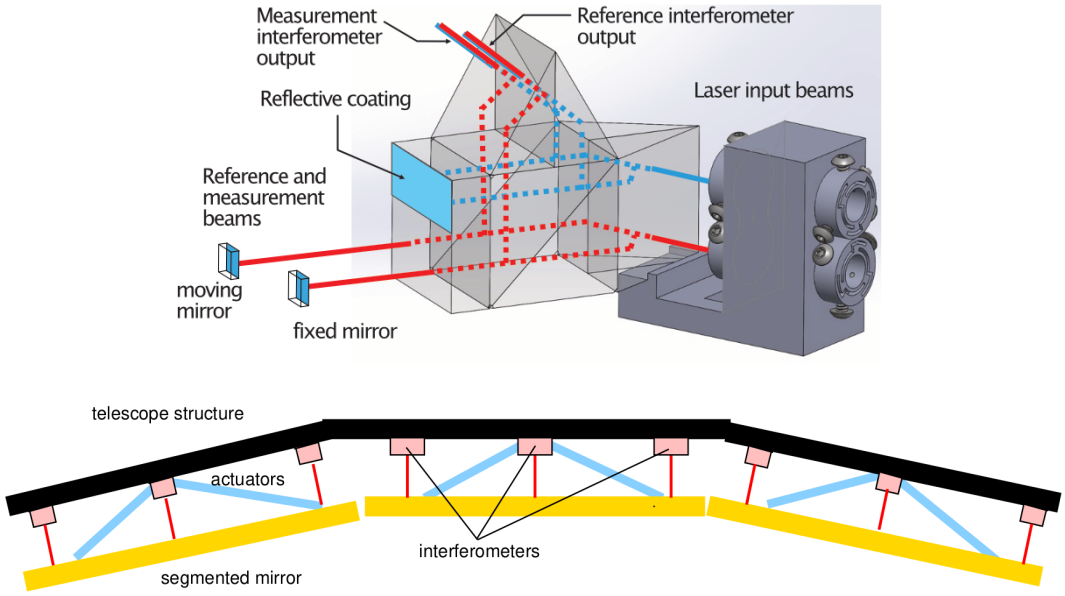

Figure 3. Top: Illustration of the beams passing through the compact interferometer. The quasi-monolithic component facilitates beam splitting and recombination of two input beams to yield two interferometric readout signals. The upper beam pair serves as one interferometer arm and is directly reflected from a highly reflective coating on the component itself, while the lower beams exit and reflect from a fixed reference mirror and the moving mirror under test, respectively. Ideally, phase signals not caused by the motion of the target object are common in both interferometers and cancel out when computing the differential phase signal. Bottom: potential implementation in a segmented telescope, where three compact interferometers per segment measure the relative position of the segmented mirror with respect to the telescope structure. Each interferometer measures distance changes and relative rotations.

The interferometers will use two laser beams with a frequency offset in the kHz to MHz range to realize two heterodyne interferometers: the reference and the measurement interferometers. The actual signal, i.e., the motion of a target object (a mirror segment) can be measured by taking the difference between the measurement and the reference interferometers. This is necessary to cancel the common phase noise coming from the lasers and fibers. The heterodyne signal will be measured with quadrant photodetectors to allow differential wavefront sensing (DWS), and thus measure the tip and tilt of the telescope's segments in addition to their translation. The signals from the photodetectors will be acquired by fast analog-to-digital converters, and their phases extracted with multi-channel phasemeters. The stability of the reference interferometer will be assessed by reflecting both outgoing beams from a single fixed mirror and computing the differential phase. This will reveal the underlying noise floor of the interferometric readout. Upscaling the system to include many sensor heads does not require additional lasers or phase-lock loop systems. The lasers are common to all the interferometers, and they can be deployed around the segments of a telescope using optical fibers.

3.4 Wavefront sensing

Real-time wavefront measurement systems have been developed in the past that are capable of reaching differential wavefront measurement resolutions below λ/2000 [21] with λ=1064 nm, corresponding to a resulting wavefront error below 3 $mrad_{RMS}$ (500 pm_{RMS} at λ=1064 nm) in a single shot measurement, with no further integration. The instrument measures the relative geometry and orientation of two interfering wavefronts in real time by using a CCD camera and retrieving the phase of the interference at each pixel.

Significant advances in CCD and CMOS camera technologies have been achieved over the past decade that will allow us to develop a highly enhanced instrument capable of achieving higher wavefront measurement rates, higher spatial resolutions, and much higher sensitivity due to the better timing performance of current cameras. Furthermore, we will also incorporate the capability of conducting extended measurement runs that will allow us to directly measure the wavefront errors in our test facility over longer integration times, consistent with the timescales (tens to hundreds of seconds) relevant for HWO.

3.5 Telescope mockup design and construction

One of the goals of the project is to test all the technologies in a representative environment and with a representative optical system, i.e., a telescope. For this reason, we will develop a mock-up telescope. We foresee fused silica mirrors and an invar spacer to realize a Cassegrain-like telescope with a primary mirror of diameter between 25 cm and 50 cm and a magnification between 10 and 50, respectively. The final design will be determined in the framework of this project. It is important to note that the goal of designing and constructing a telescope is not to demonstrate picometer wavefront error stability but to allow us to test our technologies in a relevant set-up, for this reason we anticipate that fused silica mirrors will suffice for this effort, while expediting delivery and reducing cost. While the telescope will not meet HWO requirements by orders of magnitude, differential measurements will provide good indication of the quality of our novel metrology systems and technology, e.g., one can observe wavefront changes at

the picometer level, or dimensional changes at the sub-picometer level. The telescope will be placed in a vacuum chamber with the thermal control described in previous sections. The temperature will be controlled at a few degrees above room temperature (~5°C). The position of the sensors will be defined according to simulations that will indicate the most critical positions. The goal is to obtain a temperature map that allows us to reconstruct the telescope wavefront errors. The position and number of sensors will depend on the order of the Zernike polynomials we want to recover, which in turn, will depend on the sensor levels of the temperature sensors.

Additionally, the set-up will allow us to validate and correlate models, e.g., on how the wavefront changes due to thermal fluctuations and excitations, and whether these changes are consistent with our models. Lastly, the several technologies assembled and combined in a vacuum chamber can be used to measure properties (e.g. coefficients of thermal expansion at the ppb/K level) of materials or technologies of interest for HWO.

4. Milestones, success criteria, and schedule

Given below are the anticipated tasks/work packages (WPs) related to each technology development, the associated timeline over the 3-year project duration which we divided into three months periods (quarters Q1 to Q12), and a definition of the main milestones (MS) for the work proposed here.

4.1 Thermal sensing and control

The goal is to demonstrate an environment with ultra-low temperature fluctuations and reach sensing noise levels of 1 μK/√Hz at frequencies down to 10 mHz. This is equivalent to 3 μK RMS for a frequency band from 10 mHz to 10 Hz. In terms of thermal gradients, this implies that we can resolve thermal gradients with a precision of 3 μK/Δx, where Δx is the distance between two sensors, e.g., for sensors 1 m apart we can resolve thermal gradients of 3 μK/m. While the sensing goal is set to 3 μK, the actual temperature stability goal is set to 30 μK to account for control limitations. The main milestone associated with this task is the installation of thermal sensing and control in a vacuum chamber to be procured during the project.

WP1: Design and layout of the temperature sensing system and its characterization at the μK level (Q1 to Q3):

- Define the requirements and identify components for both the analog front end (Wheatstone bridge and amplification for ADC) and the digital signal processing
- Procurement of components
- Design, procure, and populate printed circuits boards
- Test first prototype and characterize the noise performance

WP2: Design of thermal shields and active control (Q1 to Q4)

- Define requirements such as dimensions and thermal attenuation
- Complete the mechanical design of the thermal shield in Solidworks
- Design of temperature controller and identification of suitable actuators
- Procurement of parts

WP3: Assembly of thermal sensing and control (Q5 to Q6)

- Installation of the thermal shield
- Installation of the temperature sensors
- Installation of temperature actuators

WP4: Commission of the thermal sensing and control systems (Q5 to Q9)

- Closing the feedback loop for temperature control
- Measurements of temperature stability
- Optimization of control loop parameters
- Characterization of performance and thermal attenuation transfer functions

MS1 (Q9): Completion of installation of thermal sensing and control in vacuum chamber

Success criteria: 30 μK (rms) stability at room temperature demonstrated in time scales from 100 seconds to 0.1 seconds.

4.2 Picometer optical truss interferometers

The main objective is the demonstration of picometer precision with long-baseline optical truss interferometers in time scales of minutes to seconds. Achieving this will include completion of the following WPs:

WP1: Definition of cavity parameters and mechanical design (Q1-Q2)

- Optical simulations with the software Finesse to determine cavity parameters such as mirror radius of curvature, reflectivity, and cavity length to accommodate an increased operating distance
- Mechanical design (Solidworks) of updated input and return stages
- Complete optical layout of the setup
- Procurement of readily available off-the-shelf components
- Procurement of custom parts from industry partners

WP2: Table-top setup to provide input beam for one OTI (Q1-Q4)

- Plan and complete laser setup including suitable EOMs and modulation hardware
- Set up frequency stabilization and locking hardware
- Generation of high signal-to-noise ratio error signal for sideband-locking from injecting light into an auxiliary cavity

WP3: Parameter verification of OTIs and side-band locking (Q3-Q9)

- Construction of three OTIs
- Setup inside a vacuum chamber
- Characterization of OTIs including measurements of round-trip loss, cavity finesse, and mode matching efficiency.
- Comparison of actual performance with design values
- Implementation of side-band locking and retrieval of OTI stability from feedback signals

MS2 (Q9): Demonstration of picometer precision with 3-m optical truss interferometers in time scales of minutes to seconds

Success criteria: Demonstration of 1.5 pm (rms) precision measurements over a distance of 3 m in time scales from 100 s to 0.1 s.

4.3 Miniature interferometers

Our goal is to upgrade our compact interferometers to include quadrant photodetectors and differential wavefront sensing. Furthermore, we aim to simplify the geometry to reduce overall complexity, ease alignment, and increase robustness. We aim to demonstrate a quasi-monolithic beam splitting and recombination device that can sense length changes with picometer precision and beam tilt with nano-radian precision, respectively. Performance will be verified with a stable reference mirror instead of a moving object.

WP1: Update of current design (optical and mechanical) to accommodate quadrant photo detectors (Q1-Q2)

- Determine optimal quadrant photo detector (QPD) in terms of noise, material and size/speed
- Design and build custom electronics to acquire the signals of the 4 quadrants individually with low noise and high bandwidth
- Realize mechanical mount for existing quasi-monolithic interferometers to incorporate the QPD

WP2: Heterodyne laser preparation setup and phase readout system (Q1-Q4)

- Preparation of detailed optical layout of the experiment
- Procurement of components
- Commissioning of the phase readout system

WP3: Displacement and beam tilt sensing (Q4-Q8)

- Characterize performance of displacement and beam tilt sensing, respectively
- Assess frequency range, dynamic range of tilt sensing, and limiting noise levels
- Noise hunting and optimization of sensitivity

MS3 (Q8): Realization of an optical head and demonstration of picometer precision and nanoradian tilt sensing sensitivity, respectively.

Success criteria: Demonstration of a compact interferometric unit with 5 pm (rms) displacement and 30 nrad (RMS) tilt sensitivity, respectively, in time scales from 100 s to 0.1 s.

4.4 Wavefront measurement instrument

We are aiming to verify, characterize, and test a wavefront measurement system. This effort comprises the following WPs:

WP1: development of enhanced timing and triggering system on a digital signal processing (DSP) platform (FPGA board) (Q4-Q6)

- Setup heterodyne laser interferometer to generate a beat note (with adjustable frequency) which is detected with a single element photo detector
- Digitize the sinusoidal signal and process it to generate a suitable trigger signal for the camera to take images with a half-wave phase delay.

WP2: Programming, commissioning, and testing of fast camera (Q4-Q6)

- Interface camera with the triggering system
- Identify limiting parameters such as minimal exposure time, dead time, and repetition rate

WP3: Integration of DSP system and camera, and functionality tests (Q6-Q8)

- Record images and compute the per pixel phase-map
- Develop GUI for real-time phase imaging
- Determine wavefront error of resulting phase front measurements

MS4 (Q8): Verification, characterization and testing of wavefront measurement system and wavefront instrument error determination.

Success criteria: Demonstration of wavefront sensing with wavefront error below 100 pm_{RMS} at λ=1064 nm.

4.5 Final test campaign

We will test all the technologies operating together in the test facility – thermal sensing and control, optical trusses, miniaturized interferometers, and heterodyne wavefront sensors. Note we do not expect the telescope to meet the stringent HWO requirements. Nevertheless, the test campaign will be extremely useful to validate the different metrology systems in a relevant set-up. Additionally, it will allow us to correlate models (dimensional stability and WFE) to actual measurements.

WP1: Procurement of vacuum chamber (Q1-Q4)

WP2: Commissioning of vacuum chamber (Q5-Q8)

WP3: Design of telescope system (Q3-Q5)

WP4: Fabrication of mirrors and support structure (Q6-Q8)

WP5: Integration and testing of telescope and the metrology systems (Q9-Q12)

MS5 (Q12): Test campaign

Success criteria: long-term (up to 12h) measurement campaign with all technologies acquiring data simultaneously to demonstrate the suitability of the systems to characterize a telescope.

4.6 Schedule

The planned schedule for the work packages and milestones as listed above is summarized in Table 2 below.

Table 2: Schedule of the proposed work packages/activities and milestones.

Milestones (MS) / Activities		Year 1				Year 2				Year 3			
Thermal sensing and control		Q1	Q2	Q3	Q4	Q5	Q6	Q7	Q8	Q9	Q10	Q11	Q12
WP1	Temperature sensing at micro-Kelvin												
WP2	Design of thermal shields and control												
WP3	Assembly of thermal sensing and control												
WP4	Commissioning and characterization												
MS1	Thermal sensing and control in vacuum												
Optical truss interferometers													
WP1	Cavity parameters + mechanical design												
WP2	Sideband-locking error signal												
WP3	3 OTIs + performance verified in vacuum												
MS2	pm precision over minutes												
Miniature interferometers													
WP1	Update design												
WP2	Laser preparation and phase readout												
WP3	Demonstration of length and tilt sensing												
MS3	pm level length and nrad tilt sensing												
Wavefront measurement system													
WP1	Enhance timing and triggering DSP												
WP2	Testing of fast camera												
WP3	Integration of DSP system and camera,												
MS4	Wavefront measurement system verified												
Test campaign													
WP1	Procurement of vacuum chamber												
WP2	Commissioning of vacuum chamber												
WP3	Telescope design												
WP4	Fabrication of telescope components												
WP5	Integration of sensing technology												
MS5	Simultaneous testing complete												

5. Risk assessment

5.1 Sources of Uncertainties

Low frequency interferometric metrology is susceptible to a plethora of disturbances. For instance, optical trusses require a primary laser locked to a very stable frequency reference. Other sources of uncertainties come from residual amplitude modulation (RAM), which appears due to non-idealities in electro-optical modulators required in the

optical truss sensing scheme. Relative intensity noise is also a potential noise source and, thus will have to be monitored closely.

In miniaturized interferometers, there are several potential limitations that need to be addressed. We believe shot-noise will not be a limiting factor, however, technical noise sources such as relative intensity noise (RIN), photodetectors' noise (dark current and transimpedance amplifier noise), and phasemeter noise are strong candidates to limit the performance. Nevertheless, sub-picometer noise levels should be feasible.
Alignment and mechanical stability are always aspects to consider, especially at long time scales (typically for averaging times over few minutes).

For thermal sensing and control, the sources of uncertainty are related to the sensing device itself. While thermistors exhibit a high sensitivity, their long-term stability is worse compared to Platinum sensors. For the active control, it is not certain whether an asymmetric control, i.e., only with heaters will be able to reach sub-mK thermal stability levels. Finally, the thermal maps accuracy from limited locations (sensors location) is yet to be determined, which will play a role in determining thermal gradients across the primary mirror and telescope structure.

5.2 Mitigation strategies

There are several approaches to mitigate the sources of uncertainty listed above. For the optical trusses, high-finesse optical cavities instead of spectroscopy units might be needed to achieve the goal sensitivity. The combination of both is also possible if short- and long-term stability are needed. Issues related to residual amplitude modulation and technical relative intensity noise can be addressed through control loops to stabilize them. We have extensive experience in the design of low-noise electronics and can develop suitable photodiode circuits based on low-noise transimpedance amplifiers should we run into limitations due to using off-the-shelf photo detectors. Custom made circuits will allow for a tailored frequency response and allow including signal amplification, demodulation, and filtering directly on the printed circuit board, which will help with noise reduction.

For the miniaturized interferometers, some of the potential limitations can be overcome by choosing a suitable heterodyne frequency: low enough to reduce phasemeter noise (e.g., clock noise) and high enough to avoid laser's relative intensity noise. The generation of the heterodyne frequency is another free parameter that needs to be analyzed in detail. While the baseline is frequency offset phase locking, we will also consider other approaches using acousto-optical modulators (AOMs). Alternatively, other heterodyne methods are possible such as deep phase modulation [29] and deep frequency modulation [30]. While the sensitivity of these systems will not be better than classical heterodyne interferometers, they can provide simplified read-outs which might be useful when deploying a large quantity of sensing heads. Finally, if heterodyne interferometry is not sensitive enough, mini-optical cavities are an alternative to measure the relative motion of the segments of a telescope.

Regarding thermal sensing and control, we will contemplate more exotic solutions based on optical technologies (e.g., whispering galleries in photonic integrated circuits) to

measure temperature, if necessary. Similarly, we will consider actuators other than heaters, e.g., Peltier elements coupled with heat pipes to achieve a symmetric controller.

6. References

[1] Committee for a Decadal Survey on Astronomy and Astrophysics 2020 (Astro2020). "Pathways to Discovery in Astronomy and Astrophysics for the 2020s." 2023, The National Academies Press, Washington DC

[2] B. P. Crill. "The 2024 Exoplanet Exploration Program Technology Gap List", https://exoplanets.nasa.gov/internal_resources/3125/

[3] C.-P. Lajoie *et al.* "A Year of Wavefront Sensing with JWST in Flight: Cycle 1 Telescope Monitoring & Maintenance Summary." *arXiv:*2307.1119v1 (2023)

[4] J. Livas *et al.* "Telescopes for space-based gravitational wave missions". *Optical Engineering* 52(9), 091811 (September 2013)

[5] T. E. Brooks and H. P. Stahl. "Precision thermal control technology to enable thermally stable telescopes". *J. Astron. Telesc. Instrum. Syst.* 8(2), 024001-1 (2022)

[6] M. Armano et al. "Sub-Femto-g Free Fall for Space-Based Gravitational Wave Observatories: LISA Pathfinder Results." *Phys. Rev. Lett.* 116 231101 (2016)

[7] J. Sanjuan *et al*. "Thermal diagnostics front-end electronics for LISA Pathfinder" *Rev. Sci. Instrum.* 78, 104904 (2007)

[8] D. Roma-Dollase *et al.* "Resistive-Based Micro-Kelvin Temperature Resolution for Ultra-Stable Space Experiments" *Sensors* 23, 145 (2022)

[9] J. Sanjuan *et al.* "Long-term stable optical cavity for special relativity tests in space". *Opt. Express* 27, 36206 (2019)

[10] J. Sanjuan *et al.* "Carbon fiber reinforced polymer dimensional stability investigations for use on the laser interferometer space antenna mission telescope". *Rev. Sci. Instrum.* 82, 124501 (2011)

[11] J. Sanjuan *et al.* "Note: Silicon carbide telescope dimensional stability for space-based gravitational wave detectors". *Rev. Sci. Instrum.* 83, 116107 (2012)

[12] K. Jersey, I. Harley-Trochimczyk, Y. Zhang, F. Guzman. "Optical truss interferometer for the LISA telescope" *Appl. Optics* 62, 5675-5682 (2023)

[13] J. I. Thorpe, K. Numata, J. Livas "Laser frequency stabilization and control through offset sideband locking to optical cavities*" Opt. Express* 16, 15980 (2008)

[14] J. Sanjuan et al. “Simultaneous laser frequency stabilization to an optical cavity and an iodine frequency reference” *Opt. Lett.* 46, 360 (2021).

[15] K. Doeringshoff *et al.* “A flight-like absolute optical frequency reference based on iodine for laser systems at 1064 nm*” Appl. Phys.* B 123:183 (2017).

[16] G. Heinzel *et al.* “The LTP interferometer and phasemeter”. *Class. Quantum Grav.* 21, S581–S587 (2004).

[17] G. Heinzel *et al.* “Tracking Length and Differential-Wavefront-Sensing Signals from Quadrant Photodiodes in Heterodyne Interferometers with Digital Phase-Locked-Loop Readout”. *Phys. Rev. Applied D* 14, 054013 (2020).

[18] M. Armano *et al.* “Sensor noise in LISA Pathfinder: An extensive in-flight review of the angular and longitudinal interferometric measurement system” *Phys. Rev. D* 106, 082001 (2022)

[19] Charlotte E. Guthery and Michael Hart, "Pyramid and Shack–Hartmann hybrid wave-front sensor," *Opt. Lett.* 46, 1045-1048 (2021).

[20] Dali Ramu Burada, Kamal K. Pant, Mohamed Bichra, Gufran Sayeed Khan, Stefan Sinzinger, Chandra Shakher, “Experimental investigations on characterization of freeform wavefront using Shack– Hartmann sensor,” *Opt. Eng.* 56(8), 084107 (2017)

[21] Felipe Guzmán Cervantes, Gerhard Heinzel, Antonio F. García Marín, Vinzenz Wand, Frank Steier, Oliver Jennrich, and Karsten Danzmann, "Real-time phase-front detector for heterodyne interferometers," *Appl. Opt.* 46, 4541-4548 (2007).

[22] M. Armano et al. “Temperature stability in the sub-milliHertz band with LISA Pathfinder.” *Mon. Not. R. Astron. Soc.* 486 (2019).

[23] K. Jersey, Y. Zhang, I. Harley-Trochimczyk, and F. Guzman, “Design, fabrication, and testing of an optical truss interferometer for the LISA telescope,” *Proc. SPIE* 11820, 118200L (2021).

[24] R. W. P. Drever, J. L. Hall, F. V. Kowalksi, J. Hough, G. M. Ford, A. J. Munley and H. Ward. “Laser phase and frequency stabilization using an optical resonator,” *Appl. Phys. B* 31, 97-105 (1983).

[25] E. D. Black, “An introduction to Pound-Drever-Hall laser frequency stabilization,” *Am. J. Phys.* 69(1) (2001).

[26] M. Armano et al. “Sensor noise in LISA Pathfinder: An extensive in-flight review of the angular and longitudinal interferometric measurement system.” *Phys. Rev. D* 106, 2022

[27] Y. Zhang and F. Guzman, "Quasi-monolithic heterodyne laser interferometer for inertial sensing," *Opt. Lett*. 47, 5120-5123 (2022).

[28] A. Hines, A. Nelson, Y. Zhang, G. Valdes, J. Sanjuan, F. Guzman. “Compact optomechanical accelerometers for use in gravitational wave detectors,” *Appl. Phys. Lett.* 27 February 2023; 122 (9): 094101.

[29] G. Heinzel *et al.* “Deep phase modulation interferometry”. *Opt. Express* 18, 19076 (2010).

[30] O. Gerberding. “Deep frequency modulation interferometry” *Opt. Express* 23, 14753 (2015).

7. List of Acronyms

ADC	Analog-to-Digital Converter
AOM	Acousto Optical Modulator
CCD	Charge-Coupled device
CMOS	Complementary Metal–Oxide–Semiconductor
DWS	Differential Wavefront Sensing
EOM	Electro-optic Modulator
ExEP	ExoPlanet Exploration Program
FPGA	Field-programmable Gate Array
HWO	Habitable Worlds Observatory
JWST	James Webb Space Telescope
LISA	Laser Interferometer Space Antenna
NTC	Negative Temperature Coefficient
OTI	Optical Truss Interferometer
PDH	Pound-Drever-Hall
PLL	Phase-locked Loop
ppb	Parts per Billion
QPD	Quadrant Photo Detector
rms	Root mean square
TEC	Thermo-electric cooler
ULE	Ultra Low Expansion
VCO	Voltage-controlled Oscillator
WFE	Wavefront Error